PHYSICAL REVIEW B **88**, 140101(R) (2013)

Metastability and microscopic avalanche dynamics in charge-density waves of chromium

Hyekyung Clarisse Kim,[1] Jonathan Michael Logan,[1] O. G. Shpyrko,[2] P. B. Littlewood,[1,3] and E. D. Isaacs[1,3]
[1]*Department of Physics, University of Chicago, Chicago, Illinois 60637, USA*
[2]*Department of Physics, University of California San Diego, La Jolla, California 92093, USA*
[3]*Argonne National Laboratory, Argonne, Illinois 60439, USA*
(Received 16 March 2013; published 7 October 2013)

We have measured the relaxation of charge-density waves in chromium from out-of-equilibrium states achieved through rapid thermal quenching. Although pinned density waves have been predicted to relax through stick-slip dynamics, in which long-lived metastable states are linked by abrupt rearrangements of the microscopic structure, these microscopic behaviors have not been observed. Using synchrotron x rays, we have measured metastability of the order parameter and microscopic pinning phenomena including an avalanche of the charge-density wave phase. Molecular dynamical simulations based on the Fukuyama-Lee-Rice model show that these behaviors may be attributed to nucleation, pinning, and propagation of phase solitons.

DOI: 10.1103/PhysRevB.88.140101 PACS number(s): 71.45.Lr, 61.43.Bn, 75.60.Ch, 75.50.Ee

Nearly four decades since the first theories on the subject were propounded,[1] many questions still remain in the physics of elastic periodic media in random quenched disorder. The common feature of this diverse class of systems—which includes Wigner crystals,[2] vortices in high-T_c superconductors,[3] and incommensurate density waves[4]—is a corrugated energetic landscape richly populated with metastable states that are separated by finite energy barriers. This feature gives rise to fascinating behaviors such as plasticity and creep, glassy relaxation, and self-organized criticality.[5–8] Here, we report studies of the incommensurate charge-density wave (CDW) of chromium. Because incommensurate CDWs are only weakly phased to the ionic lattice, they form "soft" electronic states that can respond easily to applied perturbations. However, random disorder arising from impurities, defects, and dislocations can set the preferred phase of the CDW and produce glassy phenomenology. These effects have been observed in bulk transport properties of quasi-one-dimensional CDW compounds, for example, through current pulse and thermodynamic measurements.[9] In recent years, x-ray diffraction and topography have been used to directly measure the order parameter and shear strain profile induced by an electric field in the CDW compound $NbSe_3$.[10–12] The local distribution of impurities and defects is thought to govern the CDW domain structure[13] and pin the phase at metastable values[14] in bulk Cr, and pinning by defects such as surfaces, grain boundaries, and impurities, has also been observed in Cr films.[15–17]

In this report, we show that the CDW order parameter of bulk Cr is readily driven to a nonequilibrium state by rapid thermal quenching, and that the relaxation response may be measured with high spatial and temporal resolution using time-resolved x-ray microdiffraction. Our results show clear glassy behaviors in Cr including aging, metastability, and hysteresis following a thermal quench. We also show that the CDW phase varies on a micrometer scale to adapt to the local pinning environment, and that the buildup of strain culminates in local avalanche of phase. The various results of our study were found to be consistent with the weak pinning limit of the Fukuyama-Lee-Rice (FLR) model,[18,19] which has had considerable success in describing CDW systems. Simple one-dimensional molecular dynamical simulations based on the FLR model show good qualitative agreement with our data, which are found to be consistent with an explanation based on the launching of phase solitons across local pinning barriers in CDW domains.

Cr undergoes a weakly first-order phase transition at the Néel temperature of 311 K, below which an antiferromagnetic ordering of magnetic moments is modulated by a long-range sinusoidal spin-density wave (SDW).[20] In the magnetic phase, nested sheets of the Fermi surface of paramagnetic Cr are eliminated through the formation of an exchange-split energy gap, and this nesting condition determines the ideal SDW modulation.[21] The direction of modulation occurs along any of the three cubic axes of bcc Cr with equal probability, and the magnitude of the modulation wave vector is expressed as $Q = \frac{2\pi}{a}(1 \pm \delta)$ in reciprocal lattice units (r.l.u.). Here, the lattice parameter of Cr is $a \approx 2.885$ Å at room temperature and δ measures the incommensurability between the SDW and the atomic lattice with a smooth temperature dependence that saturates to 0.05 at 4 K.[22] The CDW is a second harmonic response of the nonmagnetic bands to the mean exchange field of the SDW and consists of a real-space modulation $\rho(r) = \rho_c + \rho_o \cos[\boldsymbol{Q} \cdot \boldsymbol{r} + \varphi(\boldsymbol{r})]$, where ρ_c is the uniform charge density, ρ_o the amplitude, and $\varphi(x)$ the phase representing local distortions from an ideally periodic wave. The modulation direction is colinear with that of the SDW and occurs at twice the magnitude of the SDW wave vector. The threefold degeneracy in the direction of $\boldsymbol{Q}$ leads to the formation of three CDW satellite pairs surrounding the allowed Bragg reflections in reciprocal space, which are accessible through x-ray diffraction. As a result, a roughly equal distribution of three orthogonal Q domains may be observed with x rays throughout an unbiased Cr crystal.[13]

Experiments were performed at Sector 8-ID-E of the Advanced Photon Source at Argonne National Laboratory, where 7.35−keV x rays were selected out with a Si(111) monochromator. For measurements of spatially averaged properties, we used an unfocused beam defined by $(200 \times 200)-\mu m^2$ slits. For local measurements, we used a 500−nm beam focused by a Fresnel zone plate and passed through an order-sorting aperture. A high-purity (99.995%) bulk Cr(111) wafer was obtained from Alfar Aesar with a Bragg (002) rocking curve FWHM of 0.03 degrees. The sample was

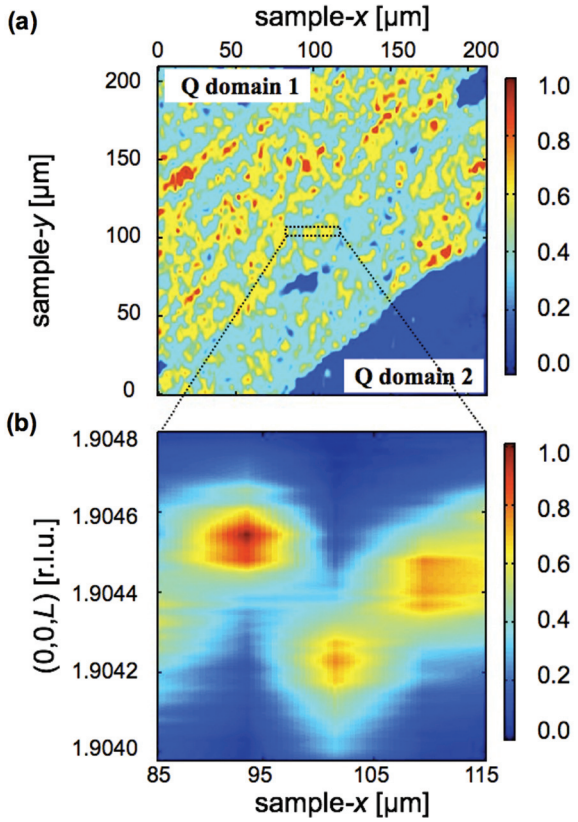

FIG. 1. (Color online) (a) Real-space map of a $(0,0,2-2\delta)$ CDW domain at 100 K with $\delta = 0.0478$. Domain 2 is oriented orthogonally to our scattering vector. (b) Reciprocal space scans at 100 K across the sample region indicated by dashed rectangle in (a).

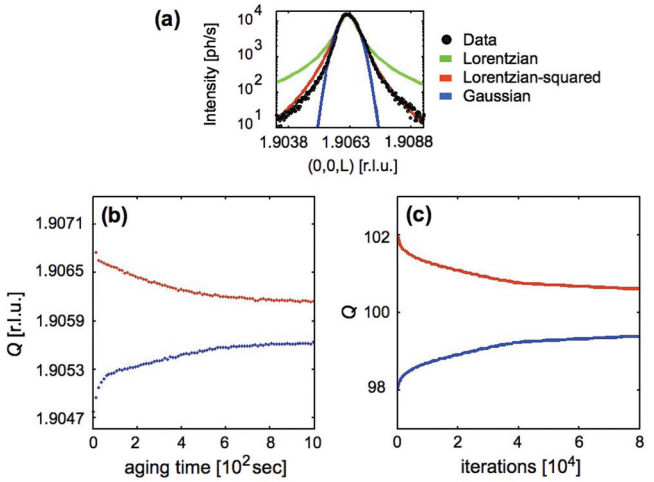

FIG. 2. (Color online) (a) Typical CDW diffraction peak following a temperature quench. Data are shown with three fits on a logarithmic scale: Lorentzian-squared (red) best fits the data with a significantly smaller chi squared than that of Lorentzian (green) and Gaussian (blue) fits. (b) Aging of Q at 150 K following thermal quench from 200 K (upper red) and from 100 K (lower blue). (c) Dynamical simulations of Q approaching the ground-state solution ($Q = 100$) from $q = \pm 2$ (red and blue lines, respectively). Solution is history dependent, saturating above and below $Q = 100$ for the different starting conditions.

mounted with GE varnish on the cold finger of a low-drift, liquid helium flow cryostat with thermal shielding provided by a beryllium dome. Following each temperature quench, stabilization at the final temperature was achieved in less than 2 minutes. Two-dimensional diffraction patterns were collected with a charge-coupled device area detector.

Figure 1(a) shows a map of CDW domains in equilibrium following 10 hours of aging at 100 K. The map was obtained through scanning x-ray microscopy with the scattering vector aligned to the $[0,0,2(1-\delta)]$ CDW satellite, where $\delta = 0.0478$ at 100 K. Scattering intensity arises from the sample region labeled Q domain 1, whose CDW modulation vector is aligned to satisfy the diffraction condition. (In the region of zero intensity, Q domain 2 is oriented orthogonally to the scattering vector.) Variations of intensity across domain 1 arise primarily from random disorder that creates differently pinned regions of CDW phase within the sample. If we scan in reciprocal space with scattering vector fixed at the average value of $\boldsymbol{Q}$, local phase deformations that lead to fluctuations in the magnitude of $\boldsymbol{Q}$ appear as variations in intensity. In Fig. 1(b), we show reciprocal space scans along $(0,0,L)$ across a small region of domain 1 indicated by a dashed rectangle in Fig. 1(a). The inhomogeneous distribution of Q values indicates that multiple phase domains constitute a single CDW domain.

A typical reciprocal space scan of the CDW superstructure measured with a large unfocused beam is shown in Fig. 2(a) along with three fits on a logarithmic scale. The best fit to our data is provided by a Lorentzian-squared line shape (red), with a significantly smaller chi squared than that of Lorentzian (green) and Gaussian (blue) fits. The phase-phase correlation decays exponentially with characteristic length $w = (3\pi^2/4)R$, where R is the average size of the so-called Lee-Rice domain beyond which phase coherence vanishes,[19] and the 3D Fourier transform leads to the ubiquitous Lorentzian-squared line shape characteristic of disordered systems.[23,24] The effects of random disorder, which dominates our phase correlation, are clearly illustrated by Fig. 2(b), where the spatially averaged order parameter is shown over aging time following a temperature quench to 150 K from 200 K (red) and 100 K (blue). The saturation of Q exhibits glassy time scales of thousands of seconds. Moreover, a striking hysteresis is observed in the final value Q_f, which depends strongly on the thermal history of the sample.

It is instructive to examine this result within the context of the FLR model of weakly pinned CDWs[18,19] for which amplitude fluctuations are assumed to be negligible below the mean-field temperature. The Ginzburg-Landau Hamiltonian for a potential that couples directly to the CDW phase consists of two competing terms representing the elastic energy of phase deformations and the interaction of the collective phason mode with the pinning potential

$$H = \int \{K[\nabla\varphi(r) - q]^2 + V\Sigma_i \cos[Qr + \varphi(x)]\delta(r - R_i)\}dx.$$

Here, $\{R_i\}$ indicate impurity positions, V the potential, K the elastic constant, and q represents perturbations that change the equilibrium value of Q to $Q + q$, as would occur naturally in a quench. The dimensionless parameter $\varepsilon = V/cK$ (c the

impurity concentration) defines the limits of weak ($\varepsilon \ll 1$) and strong pinning ($\varepsilon \gg 1$). In numerical simulations based on the FLR model, Littlewood and Rice demonstrated[25,26] that phase pinning results in metastability and stick-slip-like changes in the average phase gradient as q is monotonically increased in increments of 0.1.

Following in their steps, we performed molecular dynamical simulations using the weakly pinned ($\varepsilon = 0.1$) FLR model of a linear chain in a random distribution of 200 impurities. We looked at the effect of large perturbations ($q = 2$) that reflect the large changes in Q induced by rapid thermal quenching. After introducing a perturbation q, the phase configuration across the chain converges to a solution of minimum energy following sufficient iterations. The difference between this (final) phase configuration and the (initial) equilibrium ground state is denoted $\delta_q\varphi(r)$. The mean of the Fourier transform squared of phase information at iterative intervals yields Q over simulation time. Solutions for $q = \pm 2$ are shown in Fig. 2(c) starting at an initial value of $Q = 98$ (lower curve) and $Q = 102$ (upper curve). This simple model reproduces qualitative features of our data with both solutions saturating toward but never fully converging at the equilibrium value of 100.

In order to make the connection between bulk phenomena and the underlying microphysics, we proceeded to image the local response using a microfocused x-ray beam. First, we measured the variation of phase across a $60-\mu$m-sized CDW domain before and after a thermal quench from 150 to 100 K. The edges and spatial extent of the domain were determined by scans taken point-by-point along a line with a focused beam at fixed Q. The points at which the intensity dropped from finite to zero, corresponding to orthogonally oriented Q domains, were identified as the domain walls. Reciprocal space scans at each of 12 sample points across the domain are shown in Figure 3(a) following 12 hours of aging at 150 K. The

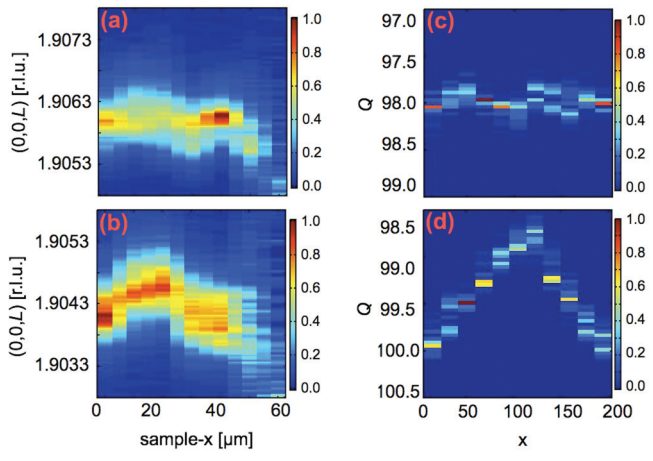

FIG. 3. (Color online) (a) Reciprocal space map of a small CDW domain at thermal equilibrium of 150 K. Values of Q are centered around 1.9061 across the domain. (b) Similar map following a quench from 150 to 100 K. Equilibration occurs heterogeneously across the domain depending on the distribution of pinning centers. (c) Simulation before perturbation with $Q = 98$. (d) Following a perturbation of $+2$, Q has converged to 100 near the ends but remains pinned at lower values with increasing distance from edge.

CDW peaks are uniformly centered around $Q = 1.9061$ r.l.u., corresponding well to values reported in the literature.[27] However, when the same domain was imaged 2 hours after a quench to 100 K [see Fig. 3(b)], the final phase configuration showed a clear spatial heterogeneity. Near the domain edges, at 0 and 60 μm, Q approaches the (lower) equilibrium value corresponding to the final temperature. As we image toward the center of the domain, particularly between 20 and 40 μm, Q remains pinned at increasingly higher values. With increasing distance from the domain wall, the CDW remains pinned in higher-energy metastable states similar to the initial phase configuration.

It is again instructive to return to the simulations with the chain ends corresponding to domain boundaries. The Fourier transform squared of the initial phase distribution, with $Q = 98$, is shown in Fig. 3(c). If we now repeat the calculation with a perturbation of $q = 2$ [see Fig. 3(d)], the final distribution of Q values is heterogeneous across the sample. Once again, Q reaches the final equilibrium value of 100 at the boundaries but remains pinned closer to the initial value of 98 toward the center of the sample. Calculations show that this effect arises from the introduction of phase slips at domain boundaries through which 2π phase solitons enter and facilitate large changes in phase. As they overcome local pinning barriers, the solitons propagate slowly inward from the edges in agreement with the results of Littlewood and Rice.[25]

By imaging a single microscopic region with time-resolved x-ray microdiffraction, we observed a local avalanche event following a quench from 4 to 200 K. We repeated measurements of Q with a time resolution of 110 s. In Fig. 4(a), an initial fast relaxation to the first metastable state Q_1 is followed by arrested dynamics at 1200 s. This state persists out to nearly 4800 s, at which point, a single avalanche takes the order parameter to a second metastable state Q_2 of a lower free energy. The width of the diffraction peak is shown over the same time interval in Fig. 4(b). When deconvolved with experimental resolution, the inverse HWHM is a measure of phase correlation, with increased broadening corresponding to increased disorder. The experimental lower bound is slightly higher than the resolution and corresponds to intrinsic narrowing of the CDW satellite peak and thus increased order. The diffraction patterns are shown in panels (i)–(iii) at the corresponding times labeled in Fig. 4(b). At time (i), the CDW is sharply peaked about Q_1. The width broadens at (ii) with decreased peak intensity immediately preceding the avalanche, and sharpens again during states of quasistable equilibrium (iii).

Switching between the two metastable states requires the introduction of phase-slip events, whereby additional phases may enter or be removed from the boundaries. CDW phase slips have been observed indirectly, for example, through steps in the temperature-dependent conductivity of $K_{0.3}MoO_3$ and orthorhombic TaS_3 whiskers.[28,29] In our direct measurement of the order parameter, the avalanche in phase allows the CDW wavelength to increase from 3.2251 to 3.2469 nm. Simulations indicate that this corresponds to the removal of a single 2π phase soliton from a phase-slip domain containing 149 CDW wavelengths, which translates to 480 nm. Thus, if the mechanism for the avalanche is the removal of a 2π soliton, then most of the region probed by the 500-nm-sized

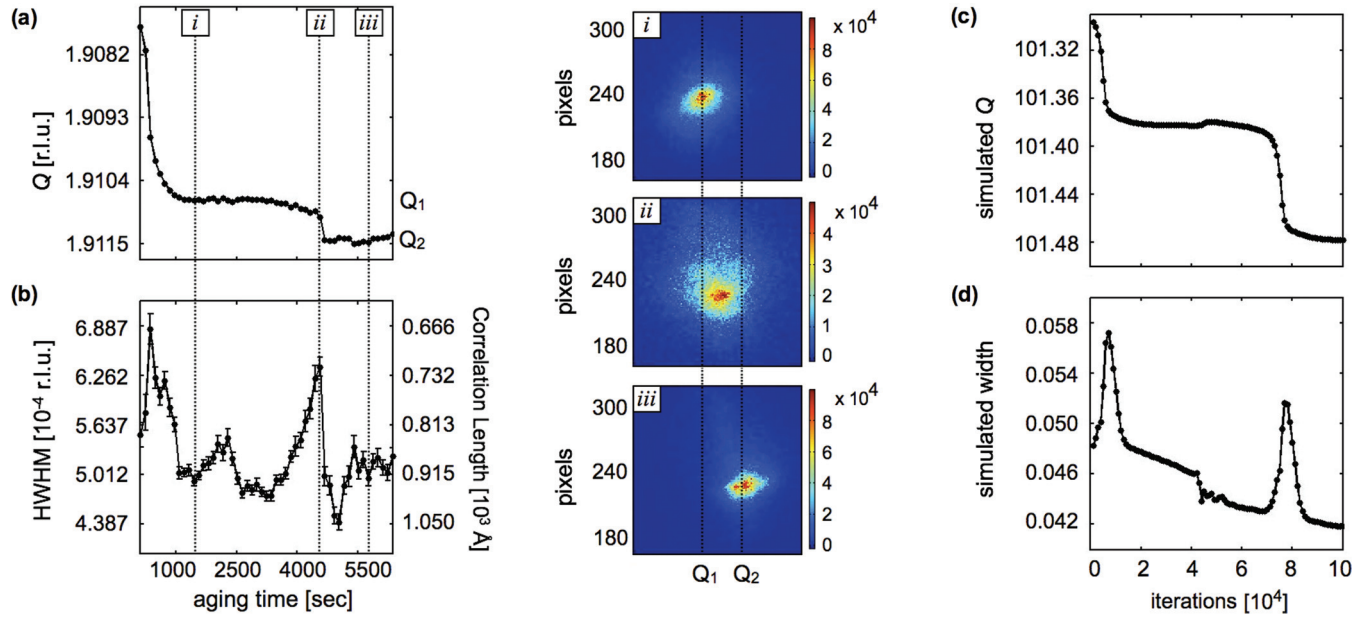

FIG. 4. (Color online) (a) Q aging at 200 K following a quench from 4 K. A fast relaxation to the first metastable state Q_1 at 1200 s is followed by an avalanche at 4800 s to a second metastable state Q_2 of lower energy. (b) Width of CDW diffraction peak over the same time interval, where peak broadening precedes the abrupt switch in Q. (i)–(iii) show diffraction patterns at the corresponding times as labeled. (c) Simulated aging of Q following perturbation from $q = 2.0$ to 2.3. Initial saturation to the first metastable state at 10^4 iterations is followed by an avalanche to a more energetically favorable state at 8×10^4iterations. (d) Simulated width of CDW peak over the same iterative interval. Simulations reproduce the avalanche and dynamical broadening and narrowing of CDW peak as seen in data.

beam is perturbed by the avalanche. Through the use of focused imaging and high time resolution, we have observed previously unresolvable behavior. To our knowledge, this is the first direct measurement of the underlying microscopic mechanisms of bulk metastability in an elastic disordered system. An additional notable feature is that in both experiment [see Figs. 4(a) and 4(b)] and simulation [see Figs. 4(c) and 4(d)], the abrupt change in order parameter is preceded by a buildup of local strain as expected from avalanche theory. Although broadening has been reported in sliding CDWs upon application of a depinning current,[30–32] the observation of dynamical broadening and sharpening of the diffraction peak for a pinned CDW at thermal equilibrium is new.

We have introduced a technique for studying nonequilibrium dynamics of CDWs by rapid thermal quenching. Illumination of single phase slip domains with high-brilliance x rays enables access to local phenomena. The key finding is that incommensurate density waves relax through stick-slip dynamics like many other natural systems such as fault gouges in the Earth's lithosphere. The kinematics of stick-slip systems is divided into a static phase, in which the object is "stuck," and a kinetic phase, in which the object is "slipping." Similarly, CDW relaxation in Cr shows long-lived metastable states punctuated by abrupt, microscopic rearrangements to states of lower free energy. Beyond providing an experimental connection between macroscopic behavior and microscopic reorderings within disordered elastic media, we foresee tremendous opportunities in the various disciplines concerned with this diverse class of systems.

Use of the Advanced Photon Source was supported by the US Department of Energy, Office of Science, Office of Basic Energy Sciences. We thank beam line scientists A. Sandy, M. Sprung, S. Narayanan, and M. Holt for their expertise and support. Use of the Advanced Photon Source was supported by the US Department of Energy, Office of Science, and Office of Basic Energy Sciences, under Contract No. DE-AC02-06CH11357. Work at the University of California, San Diego was supported by US Department of Energy, Office of Science, Office of Basic Energy Sciences, under Contract No. DE-SC0001805.

[1] A. I. Larkin, Sov. Phys. JETP **31**, 784 (1970).
[2] M. C. Cha and H. A. Fertig, Phys. Rev. B **50**, 14368 (1994).
[3] G. Blatter, M. V. Feigel'man, V. B. Geshkenbein, A. I. Larkin, and V. M. Vinokur, Rev. Mod. Phys. **66**, 1125 (1994).
[4] G. Grüner, Rev. Mod. Phys. **60**, 1129 (1988).
[5] H. Frohlich, Proc. R. Soc. London A **223**, 296 (1954).
[6] S. Brazovskii and T. Nattermann, Adv. Phys. **53**, 177 (2004).
[7] D. Le Bolloc'h, S. Ravy, J. Dumas, J. Marcus, F. Livet, C. Detlefs, F. Yakhou, and L. Paolasini, Phys. Rev. Lett. **95**, 116401 (2005).
[8] P. Bhattacharyya and B. Chakrabarti, *Modeling Critical and Catastrophic Phenomena in Geoscience: A Statistical Physics Approach* (Springer, Berlin, 2006).
[9] For an excellent review see R. E. Thorne, J. Phys. IV France **131**, 89 (2005); K. Biljakovich, J. C. Lasjaunias, O. Monceau, and F. Levy, Phys. Rev. Lett. **62**, 1512 (1989).

[10]J. D. Brock, A. C. Finnefrock, K. L. Ringland, and E. Sweetland, Phys. Rev. Lett. **73**, 3588 (1994).
[11]A. F. Isakovic, P. G. Evans, J. Kmetko, K. Cicak, Z. Cai, B. Lai, and R. E. Thorne, Phys. Rev. Lett. **96**, 046401 (2006).
[12]Y. Li, S. G. Lemay, J. H. Price, K. Cicak, K. O'Neill, K. Ringland, K. D. Finkelstein, J. D. Brock, and R. E. Thorne, Phys. Rev. Lett. **83**, 3514 (1999).
[13]P. G. Evans, E. D. Isaacs, G. Aeppli, Z. Cai, and B. Lai, Science **295**, 1042 (2002).
[14]D. W. Ruesink, J. M. Perz, and I. M. Templeton, Phys. Rev. Lett. **45**, 734 (1980).
[15]R. K. Kummamuru and Y.-A. Soh, Nature (London) **452**, 859 (2008).
[16]M. Takeda, K. Mibu, T. Shinjo, Y. Endoh, and J. Suzuki, Phys. Rev. B **70**, 104408 (2004).
[17]J. M. Logan, H. C. Kim, D. Rosenmann, Z. Cai, R. Divan, O. G. Shpyrko, and E. D. Isaacs, Appl. Phys. Lett. **100**, 192405 (2012).
[18]H. Fukuyama and P. A. Lee, Phys. Rev. B **17**, 535 (1978)
[19]P. A. Lee and T. M. Rice, Phys. Rev. B **19**, 3970 (1979).
[20]E. Fawcett, Rev. Mod. Phys. **60**, 209 (1988).
[21]A. W. Overhauser, Phys. Rev. **128**, 1437 (1962).
[22]J. P. Hill, G. Helgesen, and D. Gibbs, Phys. Rev. B **51**, 10336 (1995).
[23]S. Ravy, S. Rouziere, J.-P. Pouget, S. Brazovskii, J. Marcus, J.-F. Berar, and E. Elkaim, Phys. Rev. B **74**, 174102 (2006).
[24]Recent debate in the functional form for phase-phase correlation includes models for power law dependence in disordered flux lattices; however, the distinction between different theories resides in the tails of the correlation functions representing length scales far longer than can be observed in our experiment.
[25]P. B. Littlewood and T. M. Rice, Phys. Rev. Lett. **48**, 44 (1982).
[26]P. B. Littlewood, Phys. Rev. B **33**, 6694 (1986).
[27]D. Gibbs, K. M. Mohanty, and J. Bohr, Phys. Rev. B Cond. Matt. **37**, 562 (1988).
[28]D. V. Borodin, S. V. Zaitsev-Zotov, and F. Ya Nad', Sov. Phys. JETP **66**, 793 (1987).
[29]S. G. Zybtsev, V. Y. Pokrovskii, and S. V. Zaitsev-Zotov, Nat. Commun. **1**, 85 (2010).
[30]Y. Feng, J. Wang, R. Jaramillo, J. van Wezel, S. Haravifard, G. Srajer, Y. Liu, Z.-A. Xu, P. B. Littlewood, and T. F. Rosenbaum, PNAS **109**, 7224 (2012).
[31]R. M. Fleming, R. G. Dunn, and L. F. Schneemeyer, Phys. Rev. B **31**, 4099 (1985).
[32]K. L. Ringland, A. C. Finnefrock, Y. Li, J. D. Brock, S. G. Lemay, and R. E. Thorne, Phys. Rev. B **61**, 4405 (2000).